Natural Product Communications
June 2019: 1–7

DOI: 10.1177/1934578X19857294
journals.sagepub.com/home/npx

Cytotoxicity of New Diterpene Alkaloids, Ceylonamides G-I, Isolated From Indonesian Marine Sponge of *Spongia* sp.

Takahiro Jomori[1], Andi Setiawan[2], Miho Sasaoka[1], and Masayoshi Arai[1]

Abstract

In the course of the search for cancer cell growth inhibitors, 3 new diterpene alkaloids, designated ceylonamides G-I (**1-3**), together with ceylonamide F (**4**) were isolated from an Indonesian marine sponge of *Spongia* sp. The chemical structures of compounds **1-3** were determined using spectroscopic analysis and compared with those of compound **4**. Among the isolated compounds, **1** and **4** inhibited the growth of human prostate cancer DU145 cells in a two-dimensional monolayer culture, with an IC_{50} of 6.9 and 18.8 μM, respectively. Furthermore, these compounds are also effective on spheroid of three-dimensional cell culture model, which was prepared from DU145 cells. Based on the morphological changes in the spheroids, the minimum effective concentrations of compounds **1** and **4** were 10 and 25 μM, respectively.

Keywords

terpenoids, alkaloids, bioactivity, ceylonamide, marine sponge, cancer, spheroid, *Spongia* sp

Received: April 24th, 2019; Accepted: May 16th, 2019.

Cancer is the fastest growing health problem and leading cause of death worldwide. Although a number of new anti-cancer drugs are approved yearly, more efficacious drugs with fewer side effects are greatly needed. Natural products are the primary source of anti-cancer drugs, as about half of the present cancer therapy drugs are either natural products or their derivatives.[1] Recently, marine invertebrates such as marine sponges have emerged as a valuable resource for discovering anti-cancer drugs owing to their diverse content of secondary metabolites. Trabectedin (Yondelis) isolated from *Ecteinascidia tubinata*, and Eribulin (Halaven), a halichondrin B derivative, isolated from *Halichondria okadai* are typical examples.[2] More than 20 compounds from marine medicinal resources are in the clinical trial phase.[3] We have also isolated some marine natural products showing unique effects on the cancer cells. For instance, furospinosulin-1 (furanosesterterpene) and dictyoceratin-C (sesquiterpene phenol) are isolated from *Dactylospongia elegans*, which are selective growth inhibitors of hypoxia-adapted human prostate cancer DU145 cells.[4-7] *N*-methylniphatyne A (new 3-alkylpyridine alkaloid) and biakamides (new unique polyketides) isolated from *Xestospongia* sp. and *Petrosaspongia* sp., respectively, inhibited the growth of pancreatic cancer PANC-1 cells adapted to nutrient-starved conditions.[8,9]

On the contrary, candidate compounds with promising results in cell-based assays are often ineffective in tumor xenograft animal models, mostly due to the reliance on established two-dimensional (2D) monolayer cultures for cellular response studies. Albeit enormously useful for screening of cytotoxic compounds, the 2D monolayer culture falls short in recapitulating the complex native environment of living tumor tissue. This situation has then led to the pursuit of three-dimensional (3D) cell cultures that have the potential to improve the physiological relevance of cell-based studies and increase the successful translation of cell-based drug screening.[10] Among the 3D cell culture models, spheroid cultures are one of the well-characterized methods for screening of cytotoxic compounds due to its simplicity and reproducibility.[11]

[1] Graduate School of Pharmaceutical Sciences, Osaka University, Suita, Japan
[2] Department of Chemistry, Faculty of Science, Lampung University, Bandar Lampung, Indonesia

Corresponding Author:
Masayoshi Arai, Graduate School of Pharmaceutical Sciences, Osaka University, Yamada-oka 1-6, Suita, Osaka 565-0871, Japan.
Email: araim@phs.osaka-u.ac.jp

In this study, 3 new diterpene alkaloids, designated ceylonamides G-I (**1-3**), together with ceylonamide F (**4**) were isolated from *Spongia* sp., an Indonesian marine sponge, by bioassay-guided separation based on cytotoxic activity against 2D monolayer cultured DU145 cells. The cytotoxic effect of the compounds on 3D spheroid and 2D monolayer cultured DU145 cells was then evaluated in detail. In addition, preliminary structure activity relationship of the compounds was also discussed.

Ceylonamide G (**1**) was obtained as a white amorphous powder. The Electrospray Ionization Time of Flight Mass Spectrometry (ESI-TOF-MS) of **1** showed a quasi-molecular ion peak $[M + Na]^+$ at *m/z* 354, and the molecular formula was determined as $C_{20}H_{29}NO_3$ by high-resolution (HR)-ESI-TOF-MS. ^{1}H- and ^{13}C-Nuclear Magnetic Resonance (NMR) spectra of **1** showed the characteristic signals of terpenes, 3 methyl signals [δ_H 1.19 (3H, s), δ_C 22.4 (C-17); δ_H 1.21 (3H, s), δ_C 29.3 (C-18); δ_H 0.89 (3H, s), δ_C 14.7 (C-20)], 2 carbonyl carbon signals [δ_C 177.4 (C-16) and δ_C 183.8 (C-19)], and 2 olefin carbon signals [δ_C 129.2 (C-13) and δ_C 166.5 (C-14)]. In addition, NMR spectra of **1** were similar to those of ceylonamide F.[4,12] Marked differences in the chemical shifts of the carbon atoms in these compounds were observed at δ_C 22.8 (C-12), δ_C 129.2 (C-13), δ_C 166.5 (C-14), δ_C 45.6 (C-15), and δ_C 177.4 (C-16) for **1** and at δ_C 27.4 (C-12), δ_C 154.1 (C-13), δ_C 141.3 (C-14), δ_C 176.4 (C-15), and δ_C 49.2 (C-16) for **4** (Tables 1 and 2). Then, the Heteronuclear Multiple Bond Correlation (HMBC) correlations between δ_H 2.05, 2.32 (H-12) and δ_C 129.2 (C-13), δ_C 177.4 (C-16); δ_H 3.85, 3.95 (H-15) and δ_C 129.2 (C-13), δ_C 166.5 (C-14), δ_C 177.4 (C-16); δ_H 1.19 (H-17) and δ_C 166.5 (C-14) indicated that the γ-lactam ring of **1** had the opposite orientation to that of **4** (Figures 1 and 2). These findings and further interpretation of 2D NMR spectra, including Correlation spectroscopy (COSY) and HMBC experiments (Figure 2), led to the determination of the planar structure of **1**. All the proton and carbon signals were assigned as shown in Table 1.

Table 1. ^{1}H- (600 MHz) and ^{13}C-NMR (150 MHz) Spectral Data for Compounds **1** and **2** in CD_3OD (δ in ppm).

	1		**2**	
Position	δ_C	δ_H mult. (*J* in Hz)	δ_C	δ_H mult. (*J* in Hz)
1	41.1	0.97 td (12.9, 3.7), α 1.87 br d (12.9), β	41.1	0.96 td (13.2, 3.7), α 1.87 br d (13.2), β
2	20.2	1.46 br d (13.9), β 1.97 m, α	20.2	1.46 br d (14.1), β 1.96 m, α
3	39.2 (overlapped)	1.06 td (13.4, 4.1), α 2.13 br d (13.4), β	39.2 (overlapped)	1.06 td (13.4, 4.1), α 2.13 br d (13.4), β
4	44.7		44.7	
5	58.2	1.19 m, 1H (overlapped)	58.2	1.19 m, 1H
6	21.1	1.91 m, β 2.13 m, α	21.1	1.91 m, β 2.12 m, α
7	39.2 (overlapped)	1.39 td (13.1, 2.9), α 1.87 br d (13.1), β	39.2 (overlapped)	1.38 td (13.1, 3.0), α 1.86 br d (13.1), β
8	37.9		37.7	
9	56.8	1.18 br d (12.1), 1H	56.8	1.18 br d (12.1), 1H
10	39.2		39.2	
11	18.4	1.54 qd (12.1, 6.0), β 1.90 m, α	18.4	1.53 qd (12.4, 6.2), β 1.90 m, α
12	22.8	2.05 m, α 2.32 dd (17.4, 8.7), β	23.2	2.04 m, α 2.31 dd (17.5, 4.7), β
13	129.2		129.4	
14	166.5		163.5	
15	45.6	3.85 dq (19.7, 1.5), α 3.95 dt (19.7, 2.6), β	52.1	3.88 br d (19.4), α 3.98 br d (19.4), β
16	177.4		174.3	
17	22.4	1.19 s, 3H (overlapped)	22.5	1.18 s, 3H
18	29.3	1.21 s, 3H	29.3	1.20 s, 3H
19	183.8		181.3	
20	14.7	0.89 s, 3H	14.7	0.88 s, 3H
21			29.3	3.00 s, 3H

Table 2. ^{1}H- (600 MHz) and ^{13}C-NMR (150 MHz) Spectral Data for Compounds **3** and **4** in CD_3OD (δ in ppm).

	3		**4**	
Position	δ_C	δ_H mult. (*J* in Hz)	δ_C	δ_H mult. (*J* in Hz)
1	41.3	0.96 td (13.2, 4.0), α 1.85 m, β	41.3	0.97 td (12.6, 3.3), α 1.87 m, β
2	20.2	1.46 br d (13.8), β 1.97 qt (13.8, 4.2), α	20.2	1.46 br d (13.8), β 1.97 qt (13.8, 4.2), α
3	39.3	1.05 td (13.5, 4.3), α 2.12 br d (13.5), β	39.3	1.05 td (13.5, 4.3), α 2.12 br d (13.5), β
4	44.7		44.7	
5	58.5	1.17 br d (12.9), 1H	58.4	1.18 br d (12.9), 1H
6	20.9	1.86 m, β 2.07 br q (12.9), α	20.9	1.87 m, β 2.07 br q (12.9), α
7	37.7	1.19 m, α 2.76 dt (13.4, 3.2), β	37.7	1.19 m, α 2.75 br d (13.3), β
8	37.0		37.0	
9	57.8	1.15 br d (12.6), 1H	57.8	1.16 m, 1H
10	39.2		39.2	
11	18.7	1.52 qd (12.6, 5.7), β 1.89 m, α	18.7	1.55 qd (12.6, 5.7), β 1.88 m, α
12	27.2	2.28 ddd (18.2, 11.4, 6.6), α 2.40 dd (18.2, 5.5), β	27.4	2.29 ddd (18.5, 11.4, 6.7), α 2.40 dd (18.4, 5.4), β
13	151.6		154.1	
14	141.5		141.3	
15	173.3		176.4	
16	54.8	3.86 d (19.5), α 3.94 d (19.5), β	49.2	3.72 d (19.6), α 3.77 d (19.6), β
17	21.3	1.17 s, 3H	21.3	1.17 s, 3H
18	29.3	1.20 s, 3H	29.3	1.20 s, 3H
19	181.4		181.5	
20	14.7	0.87 s, 3H	14.7	0.87 s, 3H
21	45.6	3.48 m, 2H		
22	61.5	3.67 t (5.5), 2H		

Ceylonamide H (**2**) was obtained as a white amorphous powder. The ESI-TOF-MS of **2** showed a quasi-molecular ion peak $[M + Na]^+$ at *m/z* 368, which was larger than that of **1** by 14 amu, and the molecular formula was determined as $C_{21}H_{31}NO_3$ by HR-ESI-TOF-MS. ^{1}H- and ^{13}C-spectra of **2** were superimposed those of **1** (Table 1). The molecular formula and NMR spectra of **2** suggested that a *N*-CH_3 moiety was present in the γ-lactam ring. Indeed, the HMBC correlations were observed between δ_H 3.00 (H-21) and δ_c 52.1 (C-15), δ_c 174.3 (C-16). Further interpretation of the 2D NMR data obtained by COSY and HMBC provided the chemical structure for compound **2** as shown in Figures 1 and 2. All the proton and carbon signals were assigned as shown in Table 1.

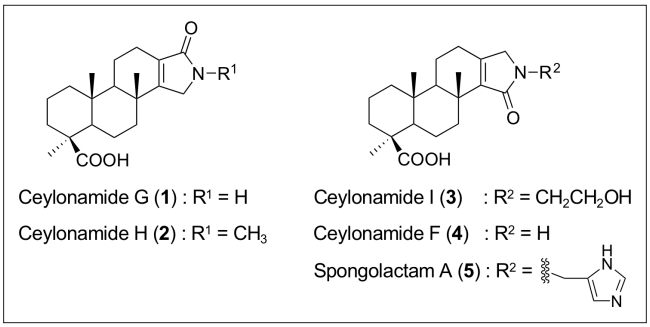

Figure 1. Chemical structures of ceylonamides **1** to **4**.

Ceylonamide I (**3**) was also obtained as a white amorphous powder. The ESI-TOF-MS of **3** showed a quasi-molecular ion peak $[M + Na]^+$ at *m/z* 398, and the molecular formula was determined as $C_{22}H_{33}NO_4$ by HR-ESI-TOF-MS. ^{1}H- and ^{13}C-NMR spectra of **3** revealed that it was similar to compounds **1**, **2**, and **4** (Tables 1 and 2). The HMBC

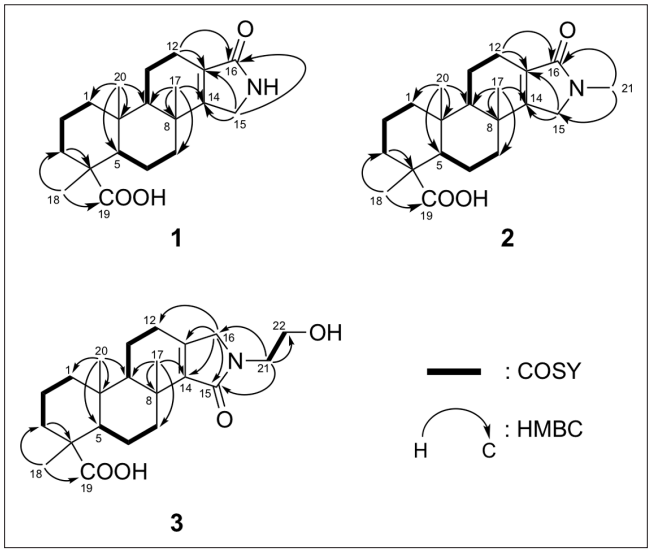

Figure 2. HMBC and COSY correlations for compounds **1** to **3**.

correlations between δ_H 3.86, 3.94 (H-16) and δ_C 27.2 (C-12), δ_C 151.6 (C-13), δ_C 141.5 (C-14), δ_C 173.3 (C-15) indicated that the γ-lactam ring of **3** was same as that of **4**. The molecular formula, the HMBC correlations between δ_H 3.48 (H-21) and δ_c 173.3 (C-15), δ_c 54.8 (C-16), δ_c 61.5 (C-22), and the COSY correlations between δ_H 3.48 (H-21) and δ_H 3.67 (H-22) revealed that a hydroxyl ethyl group was present as opposed to the unsubstituted γ-lactam ring of **4** as shown in Figure 1. All the proton and carbon signals were assigned as shown in Table 2.

The relative stereochemistry of compounds **1** to **3** was determined by analyzing their Rotating frame nuclear Overhauser effect spectroscopy (ROESY) spectra. As shown in Figure 3, the observed ROESY correlations of each compound indicated that the A/B and B/C ring junctions were both *trans* configuration, similar to ceylonamide F (**4**). The methyl group

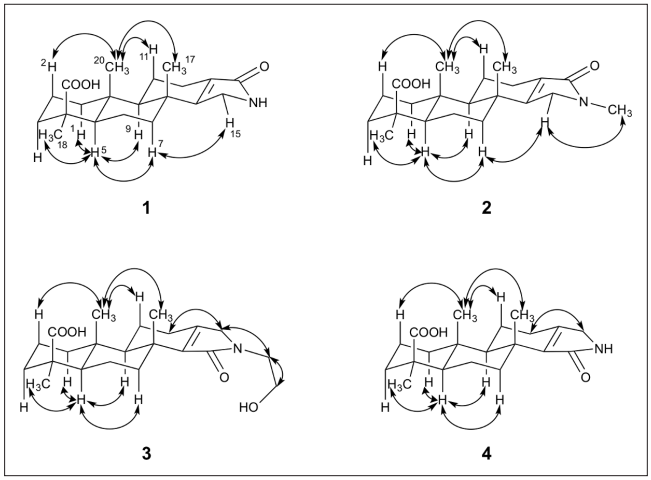

Figure 3. ROESY correlations for compounds **1** to **4**.

Table 3. Cytotoxicity of Compounds **1** to **4** Against DU145 Cells Under Two-Dimensional Culture and Spheroid.

Compounds	IC_{50} for 2D culture	MEC for spheroid
1	6.9 μM	10 μM
2	>100 μM	>100 μM
3	>100 μM	>100 μM
4	18.8 μM	25 μM
Taxol	2.6 nM	10 nM

2D, two-dimensional; MEC, minimum effective concentration.

at C-4 was assigned an equatorial orientation. As for the assignment of absolute configuration, spongolactam A (**5**), B, and C, congeners of compounds **1** to **3**, have already been elucidated by semisynthesis and their specific rotations were negative values.[13] On the other hand, the specific rotations of compounds **1** to **3** were also negative (−24, −23, and −32, respectively) and were similar to the reported specific rotations of ceylonamides A-F (−26, −29, −26, −38, −23, and −110, respectively).[12] The absolute stereochemistry of compounds **1** to **3** are illustrated in Figure 1. The absolute configuration of ceylonamide F (**4**) was also determined on the basis of the specific rotations of spongolactams.

We next evaluated the cytotoxic activity of compounds **1** to **4** on the human prostate cancer DU145 cells in 2D culture conditions. As shown in Table 3, compounds **1** and **4** showed the growth inhibition in the 2D cultured DU145 cells with IC_{50} values of 6.9 and 18.8 μM, respectively, while compounds **2** and **3** did not exhibit the activity up to 100 μM. This result suggested that there was no relationship between the activity of the compounds and the orientation of the γ-lactam ring; however, the NH group on the γ-lactam ring might be important for activity. Furthermore, the effects of compounds **1** and **4** on the spheroids prepared from DU145 cells were investigated based on the morphological changes of spheroids. In order to determine the effects of compounds, the concentrations of compounds, at which dead cells began to appear around the spheroids, were defined as the minimum effective concentration (MEC). Taxol of 10 nM concentration was used as the positive control and caused dead cells to appear at a circumference of the spheroid (Table 3 and Figure 4). On the other hand, MECs of compounds **1** and **4** were estimated as 10 and 25 μM, respectively (Table 3). Indeed, dead cells around the spheroids appeared at the concentrations shown in Figure 4. This result revealed that compounds **1** and **4** were also effective on spheroids.

Although investigating the mode of action and the effect of the compounds on the microenvironment of spheroids is necessary, our findings suggested that compounds **1** and **4** would be effective in a tumor xenograft mouse model. Hence, they are expected to be a new medicinal seed for cancer chemotherapy.

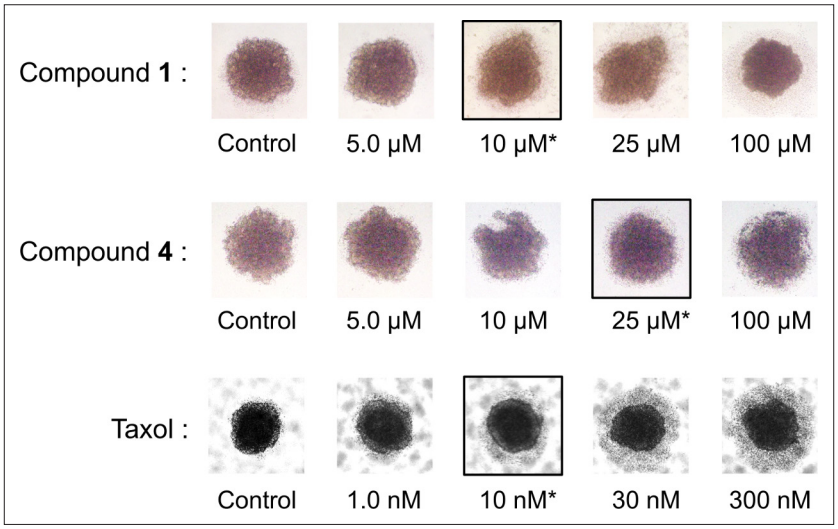

Figure 4. Effects of compounds **1** and **4** on the spheroids prepared from DU145 cells. Minimum effective concentrations of compounds **1** and **4** were determined on the basis of the morphological change in the spheroids, as described in Experimental section. Taxol was used as a positive control. "*": Minimum effective concentrations of the compounds.

Experimental

General

NMR spectra, referenced to tetramethylsilane or residual solvent peak, were measured on an Agilent NMR system (^{1}H: 600 MHz, ^{13}C: 150 MHz). ESI-TOF-MS was recorded on a Q-Tof Ultima API mass spectrometer (Waters Co., MA, United States). IR spectra and specific rotations were obtained with a JASCO FT/IR-5300 (KBr pellets) and JASCO P-2200 digital polarimeter (L = 50 mm) (JASCO Corporation, Tokyo, Japan), respectively. UV spectra were obtained with UV-2450 spectrophotometer (SHIMADZU, Kyoto, Japan). Column chromatography was performed on Silica gel BW-200 (Fuji Silysia Aichi, Japan), COSMOSIL 5C_{18}-AR-II (Nacalai tesque, Kyoto, Japan), and COSMOSIL Cholester (Nacalai tesque, Kyoto, Japan). HPLC was performed using a Hitachi L-6000 pump equipped with Hitachi L-4000H UV detector (Hitachi High-Tech Science Corporation, Tokyo, Japan). Thin-layer chromatography (TLC) analysis was carried out using pre-coated TLC plates (Merck, 60F_{254}). Spots on the TLC plates were detected by spraying acidic *p*-anisaldehyde solution (*p*-anisaldehyde: 25 mL, *c*-H_2SO_4: 25 mL, AcOH: 5 mL, and EtOH: 425 mL) or phosphomolybdic acid solution (phosphomolybdic acid: 25 g and EtOH: 500 mL) with subsequent heating. The following reagents and materials were used for cell culture and bioassay: RPMI 1640 medium (Nacalai tesque, Inc., Kyoto, Japan); fetal bovine serum (FBS; lot 30-2215) (Equitech-Bio Inc., Kerrville, TX, United States); taxol (FUJIFILM Wako Pure Chemical Corporation, Osaka, Japan); and kanamycin, 3-(4,5-dimethylthiazol-2-yl)-2,5-diphenyltetrazolium bromide (MTT), and other chemicals (Sigma-Aldrich, St Louis, MO, United States or Nacalai tesque, Inc., Kyoto, Japan).

Extraction and Isolation

The specimen of marine sponge was collected at Biak, Indonesia, and was identified as a *Spongia* sp. on the basis of morphological characteristics. The dried marine sponge of *Spongia* sp. (330 g) was extracted with MeOH. The MeOH extract (44 g) was partitioned into a water-EtOAc mixture. Following guidance of bioassay, the active EtOAc soluble portion (11 g) was subjected to silica gel column chromatography by eluting with *n*-hexane-EtOAc (10:1), EtOAc, chloroform-MeOH (10:1), and MeOH. The active chloroform-MeOH elute (0.7 g) was separated using ODS-HPLC (COSMOSIL 5C_{18}-AR-II, 10 mm i.d. × 250 mm, 60% MeOH aq. containing 0.1% trifluoroacetic acid [TFA]) to afford ceylonamide F (17.8 mg, **4**) and 6 fractions (Fr. 1-Fr. 6). The active Fr. 2 (45.5 mg) was further purified by ODS-HPLC (COSMOSIL 5C_{18}-AR-II, 10 mm i.d. × 250 mm, 55% MeOH aq. containing 0.1% TFA) to give ceylonamide G (39.4 mg, **1**). The ceylonamides H (**2**, 0.8 mg) and I (**3**, 0.8 mg) were obtained from Fr. 4 (2.1 mg) and Fr. 6 (8.6 mg), respectively, using HPLC (COSMOSIL Cholester [Nacalai tesque, Kyoto, Japan]); eluted with MeCN-H_2O containing 0.1% TFA). The ceylonamide F (**4**) was identified by ESI-TOF-MS and 2D-NMR analysis, and comparison with authentic spectral data.[12]

Ceylonamide G (1)

A white amorphous powder. $[\alpha]_D^{25}$: −24.2° (c = 0.1, MeOH). IR ν_{max} (KBr) cm^{-1}: 3276, 2928, 2848, 1693, 1452, 1213. UV λ_{max} (MeOH) nm (log ε): 217 (3.2), 223 (0.1). ESI-TOF-MS: *m/z* 354 $[M + Na]^+$. High resolution (HR)-ESI-TOF MS: Calcd for $C_{20}H_{29}NO_3Na$: *m/z* 354.2045. Found 354.2060. ^{1}H NMR (600 MHz, CD_3OD

δ_H), ^{13}C NMR (150 MHz, CD_3OD, δ_C) spectra: as shown in Table 1.

Ceylonamide H (2)

A white amorphous powder. $[\alpha]_D^{25}$: −23.1° (*c* = 0.1, MeOH). IR ν_{max} (KBr) cm^{-1}: 3326, 2898, 1672, 1522. UV λ_{max} (MeOH) nm (log ε): 216 (3.4), 222 (3.5), 225 (3.5). ESI-TOF-MS: *m/z* 368 $[M + Na]^+$. HR-ESI-TOF MS: Calcd for $C_{21}H_{31}NO_3Na$: *m/z* 368.2202. Found 368.2197. ^1H NMR (600 MHz, CD_3OD δ_H), ^{13}C NMR (150 MHz, CD_3OD, δ_C) spectra: as shown in Table 1.

Ceylonamide I (3)

A white amorphous powder. $[\alpha]_D^{25}$: −32.0° (*c* = 0.1, MeOH). IR ν_{max} (KBr) cm^{-1}: 3226, 2978, 1701, 1517. UV λ_{max} (MeOH) nm (log ε): 202 (2.8), 203 (2.8), 210 (2.8). ESI-TOF-MS: *m/z* 398 $[M + Na]^+$. HR-ESI-TOF MS: Calcd for $C_{22}H_{33}NO_4Na$: *m/z* 398.2307. Found 398.2315. ^1H NMR (600 MHz, CD_3OD δ_H), ^{13}C NMR (150 MHz, CD_3OD, δ_C) spectra: as shown in Table 2.

Cytotoxicity of the Compounds on the DU145 Cells Under 2D Culture Conditions

Human prostate cancer DU145 cells were maintained in RPMI 1640 supplemented with heat-inactivated 10% FBS and kanamycin (50 μg/mL) in a humidified atmosphere of 5% CO_2 at 37°C. In order to evaluate the activity of the compounds, the DU145 cells were plated in 96-well plates (1×10^4 cells/200 μL/well) and incubated for 12 hours in a humidified atmosphere containing 5% CO_2 at 37°C. The test compounds were later added, and the plates were incubated for an additional 24 hours under the same conditions. Cell proliferation was detected according to a previously established MTT method.[14] The growth inhibition rate was calculated as a percentage relative to negative controls. The IC_{50} values were determined by linear interpolation from the growth inhibition curve.

Spheroid Preparation and Cytotoxicity Evaluation

The preparation of spheroids from DU145 cells was performed based on the description by Friedrich et al.[11] Briefly, sterilized 1.5% agarose in RPMI 1640 medium (50 μL) was added into each well of 96-well plates, and the plates were kept at room temperature to solidify the agarose. Then, DU145 cells in the RPMI 1640 medium supplemented with heat-inactivated 10% FBS (1×10^4 cells/well/100 μL) were inoculated onto the agarose coated 96-well plates and cultured for 7 days in a humidified atmosphere of 5% CO_2 at 37°C to allow the size of spheroids to be approximately 600-700 μm. After forming spheroids, the test compounds were added, and the plates were incubated for an additional 72 hours. To evaluate the effect of the compounds on the spheroids, their concentrations that resulted in dead cells appearance around the spheroid were defined as a MEC.

Acknowledgments

This research is dedicated to the late Professor Hideaki Matsuda (Kindai University, Japan). The authors thank Dr Kazutake Tsujikawa (Osaka University) for providing DU145 cells.

Declaration of Conflicting Interests

The author(s) declared no potential conflicts of interest with respect to the research, authorship, and/or publication of this article.

Funding

The author(s) disclosed receipt of the following financial support for the research, authorship, and/or publication of this article: This research was funded by Platform Project for Supporting Drug Discovery and Life Science Research (Basis for Supporting Innovative Drug Discovery and Life Science Research [BINDS]) from AMED (Grant no. JP19am0101084), Kobayashi International Scholarship Foundation, and a Grant-in-Aid for Scientific Research B (Grant nos. 18H02096 and17H04645) from JSPS.

Supplemental Material

Supplemental material for this article is available online.

References

1. Newman DJ, Cragg GM. Natural products as sources of new drugs over the last 25 years. *J Nat Prod*. 2007;70(3):461-477.
2. Ratan R, Patel SR. Trabectedin and eribulin: Where do they fit in the management of soft tissue sarcoma? *Curr Treat Options Oncol*. 2017;18(6):34.
3. Jaspars M, De Pascale D, Andersen JH, Reyes F, Crawford AD, Ianora A. The marine biodiscovery pipeline and Ocean medicines of tomorrow. *J Mar Biol Assoc UK*. 2016;96(1):151-158.
4. Arai M, Kawachi T, Setiawan A, Kobayashi M. Hypoxia-selective growth inhibition of cancer cells by furospinosulin-1, a furanosesterterpene isolated from an Indonesian marine sponge. *ChemMedChem*. 2010;5(11):1919-1926.
5. Arai M, Kawachi T, Kotoku N, et al. Furospinosulin-1, marine spongean furanosesterterpene, suppresses the growth of hypoxia-adapted cancer cells by binding to transcriptional regulators $p54^{nrb}$ and LEDGF/p75. *ChemBioChem*. 2016;17(2):181-189.
6. Arai M, Kawachi T, Sato H, Setiawan A, Kobayashi M. Marine spongian sesquiterpene phenols, dictyoceratin-C and smenospondiol, display hypoxia-selective growth inhibition against cancer cells. *Bioorg Med Chem Lett*. 2014;24(14):3155-3157.
7. Kawachi T, Tanaka S, Fukuda A, et al. Target identification of the marine natural products dictyoceratin-A and -C as selective growth inhibitors in cancer cells adapted to hypoxic environments. *Mar Drugs*. 2019;17(3):163.
8. Arai M, Kamiya K, Shin D, et al. *N*-Methylniphatyne A, a new 3-alkylpyridine alkaloid as an inhibitor of the

cancer cells adapted to nutrient starvation, from an Indonesian marine sponge of *Xestospongia* sp. *Chem Pharm Bull*. 2016;64(7):766-771.

9. Kotoku N, Ishida R, Matsumoto H, et al. Biakamides A-D, unique polyketides from a marine sponge, act as selective growth inhibitors of tumor cells adapted to nutrient starvation. *J Org Chem*. 2017;82(3):1705-1718.
10. Kimlin LC, Casagrande G, Virador VM. In vitro three-dimensional (3D) models in cancer research: an update. *Mol Carcinog*. 2013;52(3):167-182.
11. Friedrich J, Seidel C, Ebner R, Kunz-Schughart LA. Spheroid-based drug screen: considerations and practical approach. *Nat Protoc*. 2009;4(3):309-324.
12. El-Desoky AH, Kato H, Angkouw ED, Mangindaan REP, de Voogd NJ, Tsukamoto S. Ceylonamides A-F, nitrogenous Spongian diterpenes that inhibit RANKL-induced osteoclastogenesis, from the marine sponge *Spongia ceylonensis*. *J Nat Prod*. 2016;79(8):1922-1928.
13. Mori D, Kimura Y, Kitamura S, et al. Spongolactams, farnesyl transferase inhibitors from a marine sponge: isolation through an LC/MS-guided assay, structures, and semisyntheses. *J Org Chem*. 2007;72(19):7190-7198.
14. Mosmann T. Rapid colorimetric assay for cellular growth and survival: Application to proliferation and cytotoxicity assays. *J Immunol Methods*. 1983;65(1-2):55-63.